Eur. Phys. J. C (2024) 84:1018
https://doi.org/10.1140/epjc/s10052-024-13369-2

THE EUROPEAN PHYSICAL JOURNAL C

Regular Article - Theoretical Physics

Anisotropic model observing pulsars from Neutron Star Interior Composition with modified Van der Waals equation of state

S. A. Mardan[1,a], **A. Khalid**[1,b], **Rubab Manzoor**[1,c], **Muhammad Bilal Riaz**[2,3,d]

[1] Department of Mathematics, University of Management and Technology, Lahore, Pakistan
[2] IT4Innovations, VSB-Technical University of Ostrava, Ostrava, Czech Republic
[3] Department of Computer Science and Mathematics, Lebanese American University, Byblos, Lebanon

Received: 22 August 2024 / Accepted: 15 September 2024

Abstract This paper is designed for heavy pulsars coming from the Neutron Star Interior Composition Explorer. The research model is describe by Einstein field equations for anisotropic fluid configuration with spherical symmetry. As per present perceptiveness, modified non-linear Van der Waals equation of state is used to relate physical variables. The continuity of inner and outer matter is obtained by comparing inner spacetime to outer Schwarzschild metric. The physical viability of this model is evaluated and further it is compared with observational data of pulsars PSR J0348+0432, PSR J0740+6620 and PSR J0030+0451. The model fulfils all physical and mathematical characteristics of the dense structure studies. It offers the factual proofs carried by evolution of celestial configurations. The working model presented here is physically viable and shows stable behaviour.

1 Introduction

In galaxies, dust and gas clouds having uneven distribution of matter assembled in shape of stars. Nuclear fusions of these energetic objects along with always present gravity results into celestial doom, which cause formation of hot and dense objects. Chandrasekhar [1] evaluated stellar formation of compact dense objects. Oppenheimer and Volkoff [2] reviewed the celestial object in the phase of high pressure inside of star with the help of a cold Fermi gas equation of state (EoS). Wentzel [3] governed the relationship between density dispensation and magnetic field of dense object. Kumar et al. [4] presented the static celestial equilibrium configuration of dense objects by means of simple transformation. Kumar and Bharti [5] discussed the history of dense matter and worked on modeling of dense stars. Alho et al. [6] explained that stellar dense objects, which are commonly taken as self gravitating objects are viable, radially stable and symmetrical. Astashenok et al. [7] studied compact objects involving dark energy and dark matter by applying EoS compatible for cosmological examinations.

Candelas [8] talked over vacuum polarization caused through gravity in outer area of Schwarzschild black hole to understand the Unruh vacuum, where visible observable values are finite. According to general relativity (GR), 4D is the outer spacetime of spherical non rotating star, which defines unique line element that is known as Schwarzschild metric. Candelas and Howard [9] studied the Hartle-Hawking vacuum for external zone of Schwarzschild space-time. They also provided the algebraic and rational estimated data of this model. Schwarzschild [10] delivered the fundamental answers of queries related to Schwarzschild. The answers given by him are realistic and uniform in entire space-time. Leon [11] presented celestial models with two different outer metric cases of Schwarzschild vacuum and non-Schwarzschild vacuum. Crater [12] calculated the Einstein field Equation in purpose of clarifying the Schwarzschild metric as vacuum state. Cataldo [13] used Schwarzschild metric to compute conventional derivation of Einstein Equation and Schwarzschild radius to find vacuum field. Weinstein [14] investigated the main participation of Schwarzschild in GR by obtaining inner and outer keys of compact stars by Schwarzschild metric.

Van der Waals (vdW) EoS captivated the interest of researchers due to its modest and adaptable properties. Malaver [15] expended the study of anisotropic dense realis-

[a] e-mail: syedalimardanazmi@yahoo.com
[b] e-mails: ayeshakhalid4238@gmail.com; S2019109012@umt.edu.pk (corresponding author)
[c] e-mail: rubab.manzoor@umt.edu.pk
[d] e-mails: muhammad.bilal.riaz@vsb.cz; bilalsehole@gmail.com

Published online: 08 October 2024

tic stars to solve Einstein-Maxwell system of equations with vdw EoS and inquired its charged density singularity. Jantsch et al. [16] tested the characteristics of general cosmological fluid space with vdw EoS. Further, posterior parametric values are used for vdw EoS as reported by asymptotic attitude of physical parameters. Kontogeorgis et al. [17] elaborated the history of vdw EoS and the emphasise on the need of why vdw EoS is necessary. Fleming [18] explained that how vdw EoS is related to torque shifting, which orderly made all the motion uniform in quantum field frame. Errehymy et al. [19] solved problems by choosing modifies vdw EoS in nonlinear state and find exact realistic solutions for model. Ditta et al. [20] focused on dense objects related to electric field and plotted models in $f(Q)$ gravity with vds EoS in modified state. Mustafa et al. [21] researched Einstein field equations as revised matter source with the intention of achieving results of Wormhole.

The story begins 50 years ago, when researchers get awareness of pulsars. A radio object that is pulsating named as neutron star. This discovery get attention in field of fundamental physics, GR, particle physics, and many other areas of physics. Lattimer and Prakash [22] described ideal astrophysics for proofing theories of compact neutron object as hyperon- dominated matter, superconductivity with critical temperatures and deconfined quark matter. Damour [23] represented relativistic gravity for binary pulsars and gave satisfying results of strong-field regime. Burnell and Jocelyn [24] talked about coincidental finding of pulsars and try to grow our knowledge about these compact dense matter objects. Mann [25] worked on hidden secrets of universes dark objects such as neutron-star to make people understand this natural phenomena. Zhang et al. [26] defined neutron star revolving in high magnetic field while dealing with machine learning. Reardon et al. [27] observed powerful binary neutron stars and listed features of these binary radio pulsars in 3D orbits. Farrell et al. [28] presented study on different phases neutron stars, tidal deformability, pulsar glitches, the equation of state, fast pulsars, and strange quark matter stars.

Anisotropic fluid plays a vital role in composition of self gravitating compact stars. In some cases anisotropic fluid is considered to be physically attached with inner structure of neutron stars and dense objects. Herrera et al. [29] used specific EoS to find adiabatic index for anisotropic shpere having various grades of anisotropy. Herrera et al. [30] examined the effects of one-parameter set of conformal motions considering anisotropic matter distribution and calculated analytical solutions of the Einstein equations. The reasons for appearance of anisotropy in highly dense systems are the (a) presence of magnetic field; (b) fusion of monotonic gases, electrons, molecular and ionized hydrogen, which forms anisotropic fluid; (c) anisotropic velocity dispensation in collision-less system; (d) slow revolving system; (e) effects of radiation flow going in and out in the cloud. Herrera and Santos [31] answered the questions that arise about existence of anisotropy and what are the basic properties, which shows anisotropic system is different from the isotropic system?. Which is further differentiated by the relationship between radial and tangential pressure as $p_r \neq p_t$ in anisotropic fluid and $p_r = p_t$ in isotropic fluid. Hernandez and Nunez [32] unveiled the possibility to earn reliable anisotropic symmetric configurations appearing out of density contour and EoS. Maurya and Gupta [33] exhibited a new class of restrained anisotropic high-dense objects by means of charged fluid dispensation where anisotropy parameter reaches 0. Sah and Chandra [34] shaded light on electrically independent anisotropic static fluid in solving relativistic Einstein's field equations that are non negative finite. Boonserm et al. [35] argued on unsuccessful mimicking of relativistic anisotropic sphere by appropriate linear mixture of theoretically enchanting and easy traditional matter. Tello-Ortiz et al. [36] derived analytic Einstein's field equations with anisotropic fluid distribution to accomplish embedding class framework by applying Karmarkar's condition. Herrera [37] founded that destructive fluxes, nonuniform energy densities and shear in fluid flow all work to abandon the isotropic configuration and create anisotropy in pressure. Cadoni et al. [38] used anisotropic fluid to explain dark energy world. He clarified his work with the explanation of baryonic substance, dark world and the relationship between them in absence of dark matter. Naidu et al. [39] talked over the association of anisotropic fluid causing firm electromagnetic fields which further provide thermodynamics to dense objects.

"Explorer Mission of Opportunity" that was carried out by NASA presented the work on "Neutron star Interior Composition Explorer" (NICER). The NICER involves the survey on topics like unusual gravitational field, electromagnetic, and nuclear-physics surroundings illustrated by neutron stars. Gendreau et al. [40] suggested that NICER will explain the strange matter state of dense neutron objects with high values of density and pressure. Gendreau et al. [41] pointed the importance of NICER in chapter C, "Design and Developmentv" and executed the NICER's fundamental subsystems, outlines the accomplishment that was effectively activated. Bogdanov et al. [42] showed new momentum and spectral evaluation of two dense stars taken as pulsars in X-rays stated by knowledge of NICER. Yunes et al. [43] focused on core part of quark matter by gathering information of NICER. Devarshi et al. [44] collected facts from NICER to deal with relativistic ray-tracking of thermal X-ray photons emitting from neutron stars.

The convenient way to deal with algebraic solutions describing physical conditions, is to take physical variables as metric and generating functions. In the derivation of solutions for static symmetric anisotropic fluid distribution the generating functions are important. Rahman and Visser [45] introduced an assessable monotone generating function and

exhibited Goldman-I exact solutions. Lake [46] generated every regular perfect-fluid solutions of Einstein's equations and deal with restricted generating functions to evaluate physical solutions. Herrera et al. [47] constructed an algorithm and described three known situations involving generating functions. Thus, the physical solutions of this model are evaluated by two generating functions (vdu EoS (p_r) *and* $Z(x)$).

2 Spherically symmetric metric tensor with Einstein field equations

This section presents spherically symmetric model with anisotropic fluid distribution respecting the raising function carried out by vdw EoS. Therefore, we initiate with static symmetric framework, which is given as metric tensor

$$ds^2 = e^{\nu(r)}dt^2 - e^{\lambda(r)}dr^2 - r^2(d\theta^2 + sin^2\theta d\phi^2), \tag{1}$$

where, the above metric is taken in Schwarzschild coordinates $x^a = (t, r, \vartheta, \phi)$. In this ν and λ both are gravitational potential that are functions of r, and $d\Omega_2^2 = d\vartheta^2 + \sin^2\vartheta d\varphi^2$ draws the metric of two sphere.

$$-8\pi T_{ij} = G_{ij}, \tag{2}$$

here T_{ij} is the energy-momentum tensor and G_{ij} is the Einstein's tensor for matter distribution. Moreover, the G_{ij} further presented as the relationship between Ricci tensor R_{ij} and ricci scalar R as below

$$R_{ij} - \frac{1}{2}Rg_{ij} = G_{ij}, \tag{3}$$

in above expression g_{ij} is the metric tensor. Assuming the case of matter participation in the dispersion of anisotropy. By utilizing the whole function, we gain the following equation of energy-momentum tensor.

$$T_{ij} = (\rho + p_t)u_i u_j - p_t g_{ij} + (p_r - p_t)S_i S_j, \tag{4}$$

although u^i is known as fluid four-speed and S_i is the spacelike vector where $u^i S_i = 0$. The Eq. (4) offers the elements of anisotropic T_{ij} everywhere in the shape of density ρ, radial pressure p_r, and transverse pressure p_t. This shows the simple metric element of T_{ij} stated as

$$T_{ij} = 0 \quad if \quad i \neq j. \tag{5}$$

From the Eqs. (1) and (4), we calculated Einstein field equations with $8\pi G = c = 1$, declared as

$$\rho = \left[\frac{1}{r}\frac{d\lambda}{dr} - \frac{1}{r^2}\right]e^{-\lambda} + \frac{1}{r^2}, \tag{6}$$

$$p_r = \left[\frac{1}{r}\frac{d\nu}{dr} + \frac{1}{r^2}\right]e^{-\lambda} - \frac{1}{r^2}, \tag{7}$$

$$p_t = \left[\frac{1}{2}\frac{d^2\nu}{dr^2} + \frac{1}{4}\left(\frac{d\nu}{dr}\right)^2 - \frac{1}{4}\frac{d\nu}{dr}\frac{d\lambda}{dr} + \frac{1}{2r}\frac{d\nu}{dr} - \frac{1}{2r}\frac{d\lambda}{dr}\right]e^{-\lambda}. \tag{8}$$

The group of Eqs. (6–8) explains the self gravity in anisotropic stellar configuration. The self-gravitational mass in the static spherical symmetric star with radius r is,

$$m(r) = 4\pi\int_0^r \rho r^2 dr, \tag{9}$$

Now, by applying transformations [44] subsequent set of equations are formed.

$$x = r^2, \quad Z(x) = e^{-\lambda}, \quad y = e^{\nu}, \tag{10}$$

The celestial set of Einstein field equations are (11–13)

$$\rho = \left(\frac{1-Z}{x}\right) - \frac{1}{\sqrt{x}}\frac{dZ}{dx}, \tag{11}$$

$$p_r = \left(\frac{Z-1}{x}\right) + \frac{Z}{y\sqrt{x}}\frac{dy}{dx}, \tag{12}$$

$$p_t = \left[\frac{Z}{2y}\frac{d^2y}{dx^2}\right] + \left[\frac{Z}{4} + \frac{Z}{2\sqrt{x}} - \frac{Z}{4y}\frac{dy}{dx}\right]\frac{1}{y}\frac{dy}{dx} + \frac{1}{\sqrt{x}}\frac{dZ}{dx}. \tag{13}$$

So, the $m(r)$ from Eq. (9) alter to

$$m(x) = 4\pi\int_0^x \rho x dr, \tag{14}$$

as function of x in Eq. (14). Compiling the points that a visible fluid dispensation of matter hoped to satisfy the barotropic EoS ($p_r = p_r(\rho)$). Implicating this we give thought to the inner matter dispensation that adhere to altered form of Van der Waals EoS like this,

$$p_r = \alpha\rho^2 + \frac{\beta\rho}{1+\gamma\rho}, \tag{15}$$

For the purpose of effective realization of celestial set of Eqs. (11–13) is defined. In this parameters like α,β and γ are discussed. The retardation and rapid age are clarified by constants of EoS and are bounded with conditions $\alpha, \gamma \to 0$, which can restore the dark energy EoS, along $\beta = p_r/\rho < -1/3$. It was already noticed that the perfect fluid EoS $p_r = \beta\rho$ shows an approximation of cosmic era of static environment, by taking phase changes unimportant [48]. Accordingly, the altered form of vdw EoS has the benefits of illustrating the changes from matter field controlled by scalar field except addressing the scalar field. Also, it needs the explanation from cosmos with little help of components

and vdw fluid which surely deals with dark energy and matter regarding as the only fluid. By avoiding the unbounded parameters [49], the new form of vdw chain was too productive for broad area of noticed examinations. Conversely, this kind of vdw EoS [19] is low commercial to notice the examination, and extra adjustable with complimentary parameters. As well, its believable to type the stellar set of Eqs. (11–13) in the easy form.

$$e^{\lambda} = Z^{-1}, \tag{16}$$

$$y = e^{\nu}, \tag{17}$$

$$\rho = \left(\frac{1-Z}{x}\right) - \frac{1}{\sqrt{x}}\frac{dZ}{dx}, \tag{18}$$

$$p_r = \left(\frac{Z-1}{x}\right) + \frac{Z}{y\sqrt{x}}\frac{dy}{dx}, \tag{19}$$

$$p_t = p_r + \Delta, \tag{20}$$

$$\Delta = \left[\frac{Z}{2y}\frac{d^2y}{dx^2}\right] + \left[\frac{Z}{4} - \frac{Z}{2\sqrt{x}} - \frac{Z}{4y}\frac{dy}{dx}\right]\frac{1}{y}\frac{dy}{dx} + \frac{1}{\sqrt{x}}\frac{dZ}{dx} - \frac{Z-1}{x}, \tag{21}$$

by the anisotropic equation ($\Delta = p_t - p_r$), we arranged the next expression

$$y = exp^{\int\left[\frac{\sqrt{x}}{Z}\left[a-bx+\alpha\rho^2+\frac{\beta\rho}{1+\gamma\rho}\right]\right]dx}, \tag{22}$$

now, by putting values from Eq. (10) into Eq. (1), we write the following equation,

$$ds^2 = exp^{\int\left[\frac{\sqrt{x}}{Z}\left[a-bx+\alpha\rho^2+\frac{\beta\rho}{1+\gamma\rho}\right]\right]dx}dt^2 - Z^{-1}dr^2 - r^2(d\theta^2 + sin^2\theta d\phi^2). \tag{23}$$

Thus, the results shows static symmetric anisotropic distribution along particular vdw EoS that is created for specific gravitational potential Z(x). Then, we put more information about anisotropic dense object celestial configurations.

3 Realistic results for anisotropic dense celestial form

The group of Einstein field equations that are (16–21), provided the 6 equations involving free variables ρ, p_r, p_t, Δ, y and Z. In contrast, the celestial set of equations are not independent on the gravitational potential. However, this way presents the acceptable method to show the integration steps from Eq. (21) that is the main equation in this work whose result give the Eq. (22). For this the relation of gravitational potential $Z(x)$ is stated as

$$Z = 1 - ax + bx^2, \tag{24}$$

here, a and b are free real parameters. At $x \to 0$ the $Z(x) = 1$, this gives the idea of wide range of parametric values for a and b. This $Z(x)$ is uniform, non negative and non singular at the center. As well as, it adjusts with celestial inner and fulfills every conditions to proof fundamental visible achievement. By putting Eq. (24) into Eq. (22), the following equation is formed

$$y = exp^{\int\left(\frac{d_1x^{\frac{4}{2}}+d_2x^{\frac{3}{2}}+d_3\sqrt{x}}{1-ax+bx^2}\right)dx}. \tag{25}$$

Here $P_1 = a\left(1+\frac{1}{\sqrt{x}}\right)$, $P_2 = -b\left(1+\frac{2}{\sqrt{x}}\right)$, $d_1 = 2\alpha P_1P_2$, $d_2 = 2\alpha P_1P_2 - b + \frac{\beta P_2}{1+\gamma(P_1+P_2x)}$, $d_3 = a + \alpha P_1^2 + \frac{\beta P_2}{1+\gamma(P_1+P_2x)}$. So the realistic model for stellar group of Eqs. (16–21) made up of density, radial pressure and tangential pressure is given as

$$e^{-\lambda} = 1 - ax + bx^2, \tag{26}$$

$$e^{-\nu} = exp^{\int\left(\frac{d_1x^{\frac{4}{2}}+d_2x^{\frac{3}{2}}+d_3\sqrt{x}}{1-ax+bx^2}\right)dx}, \tag{27}$$

$$\rho = P_1 + P_2x, \tag{28}$$

$$p_r = \alpha\rho^2 + \frac{\beta\rho}{1+\gamma\rho}, \tag{29}$$

$$p_t = p_r + \Delta, \tag{30}$$

so, by solving Eqs. (21) and (24), the anisotropic factor is shaped as

$$\Delta = \left[\frac{1-ax+bx^2}{2y}\frac{d^2y}{dx^2}\right] + \left[\frac{1-ax+bx^2}{4} - \frac{1-ax+bx^2}{2\sqrt{x}} - \frac{1-ax+bx^2}{4y}\frac{dy}{dx}\right]\frac{1}{y}\frac{dy}{dx} + \frac{-a+2bx}{\sqrt{x}} - \frac{1-ax+bx^2-1}{x}, \tag{31}$$

in this y is defined by Eq. (25).

Here 2 conditions os anisotropy is defined

- $\Delta < 0$, attractive in nature.
- $\Delta > 0$, repulsive in nature.

4 Matching requirements for anisotropic dense star solution

At the celestial star surface, the inner spacetime is fluently associated to the outer Schwarzschild vacuum ($r = R_s$). The relationship between mass M and radius R_s of dense object is $R_s > 2M$. Under these circumstances, the metric tensor for the celestial configuration at the junction surface Σ with radius r is

$$ds_+^2 = -\left(1-\frac{2M}{r}\right)dt^2 + -\left(1-\frac{2M}{r}\right)^{-1}dr^2 + r^2d\Omega_2^2. \tag{32}$$

On the board, the entire mass of star is M. But the below conditions must be fulfilled at the hypersurface to make sure of the fluency and regularity of inner spacetime tensor ds_-^2 and outer spacetime ds_+^2 at the surface outline.

$$[ds_-^2]_\Sigma = [ds_+^2]_\Sigma, \quad [K_{ij-}]_\Sigma = [K_{ij+}]_\Sigma, \tag{33}$$

$$e^{\nu^-}|_{r=R_s} = e^{\nu^+}|_{r=R_s} \quad and \quad e^{\lambda^-}|_{r=R_s} = e^{\lambda^+}|_{r=R_s}, \tag{34}$$

plus

$$\left(\frac{\partial e^{2\nu^-}}{\partial r}\right)_{|r=R_s} = \left(\frac{\partial e^{2\nu^+}}{\partial r}\right)_{|r=R_s}. \tag{35}$$

The inner and outer spacetimes are denoted by $-$ and $+$. Although, the K_{ij} is the curvature. By 1st fundamental form's regularity the $[ds^2]_\Sigma = 0$. where $[F]_\Sigma \equiv F(r \longrightarrow R_s^+) - F(r \longrightarrow R_s^-) \equiv F^+(R_s) - F^-(R_s)$. Plus, the sequence give following equation,

$$g_{rr}^-(R_s) = g_{rr}^+(R_s) \quad and \quad g_{tt}^-(R_s) = g_{tt}^+(R_s). \tag{36}$$

Accordingly, the Eq. (1) must satisfy the 2nd fundamental equation K_{ij} for hyper surface. And that is equal to O'Brien and Synge matching conditions [50]. Here it is discussed that p_r is zero at surface where $r = r_\Sigma$

$$p_r(R) = 0. \tag{37}$$

The celestial form size is calculated from this condition of $\sum_-$ and $\sum_+$ as inner and outer sectors. The hyper surface is defined as

$$ds^2 = d\tau^2 - R_s^2 d\vartheta^2 + R_s^2 \sin^2\vartheta d\phi^2. \tag{38}$$

The appropriate time outline is τ. In this the outlines' extrinsic curvature $\sum$ is

$$K_{ij}^\pm = -\eta_k^\pm \frac{\partial^2 y_\pm^k}{\partial n^i n^j} - \eta_k^\pm \Gamma_{\mu l}^k \frac{\partial y_\pm^\mu}{\partial n^i}\frac{\partial y_\pm^l}{\partial n^j}, \tag{39}$$

now, n^i is the coordinates of $\sum$ and $\eta_k^\pm$ is the 4-velocity of $\sum$. The elements of this 4-velocity are gained by coordinates $(y_\pm^\nu)$ of $\tau^\pm$ as below,

$$\eta_k^\pm = \pm\frac{df}{dy^k}\left|g^{\mu l}\frac{df}{dy^\mu}\frac{df}{dy^l}\right|^{-1/2} \quad with \quad \eta_k\eta^k = 1. \tag{40}$$

The inner and outer sectors with unit normal vectors are

$$\eta_k^- = [0, -e^\lambda, 0, 0] \quad and \quad \eta_k^+ = \left[0, \left(1 - \frac{2M}{r}\right)^{-1}, 0, 0\right]. \tag{41}$$

Now, by Eqs. (1) and (38) in collaborations with the Schwarzschild vacuum Eq. (32), we obtain

$$\left[\frac{dt}{d\tau}\right]_\Sigma = [e^\lambda]_\Sigma = \left[\left(1 - \frac{2M}{r}\right)^{-1}\right]_\Sigma, \tag{42}$$

the $[r]_\Sigma = R_s$. By Eq. (41) the following expressions are formulated and nonzero of them are written below, $K_{00}^- = \left[\frac{\nu'}{2}e^\nu\right]_\Sigma$, $K_{11}^- = r$, $K_{22}^- = r\sin^2$, $K_{00}^+ = \left[\frac{M}{r^2}\right]_\Sigma$, $K_{11}^+ = r$, $K_{22}^+ = r\sin^2\theta$, where$[K_{11}^-]_\Sigma = [K_{11}^+]_\Sigma$

$$e^{-\lambda} = \left(1 - \frac{2M}{R}\right). \tag{43}$$

By taking $[K_{00}^-]_\Sigma = [K_{00}^+]_\Sigma$, we get,

$$\nu'(R_s) = \frac{2M}{R_s(R_s - 2M)}. \tag{44}$$

At the hyper surface, the apropos standard show availability by Eqs. (42–44)

$$e^{\lambda(R_s)} = \left[\frac{1 - 2M}{R_s}\right]^{-1} = 1 - aR_s + bR_s^2, \tag{45}$$

$$e^{\nu(R_s)} = \left[\frac{1 - 2M}{R_s}\right] = y(R_s). \tag{46}$$

5 Graphical representation

In this section, the physical suitability of the celestial star model results are studied graphically. Currently here different physical aspects of dense star creation are focused and we developed that the results are physically possible. The recorded data of 3 dense stars $PSRJ0348 + 0432$, $PSRJ0030 + 0451$ and $PSRJ0740 + 6620$ is modeled to discuss anisotropic reaction along static symmetry inside spacetime tensor of GR. The figures are plotted by choosing suitable parametric values after compulsory factual fixing that are listed below in Tables. The selection of these parametric values are based on the physically logical requirements:

- **Required standards for density and pressure elements:** Starting with Figs. 1 and 2, its visible that density ρ_c and pressure p_c are repetitively reducing towards the exterior outline of the celestial configurations, possessing utmost values at the center of dense objects. The p_r, faded at the boundary of every celestial configuration $r = R_s$. Along the surface of dense objects, matter density is continually non negative. The ρ at the center of

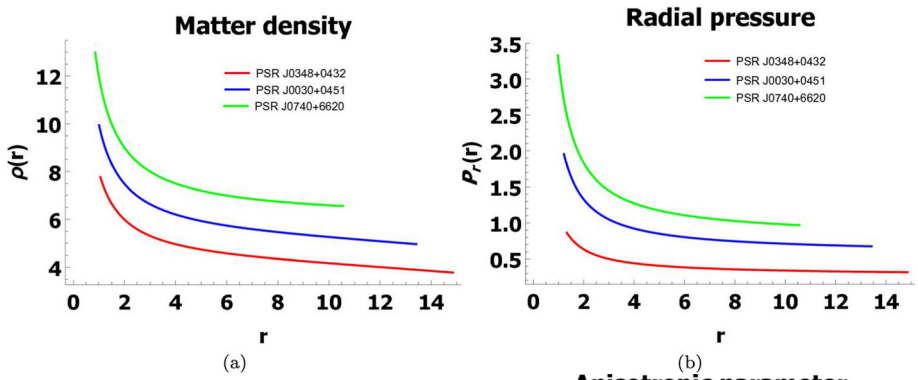

Fig. 1 Relationship of density and radial pressure w.r.t radial coordinate r. Observations of 3 pulsar

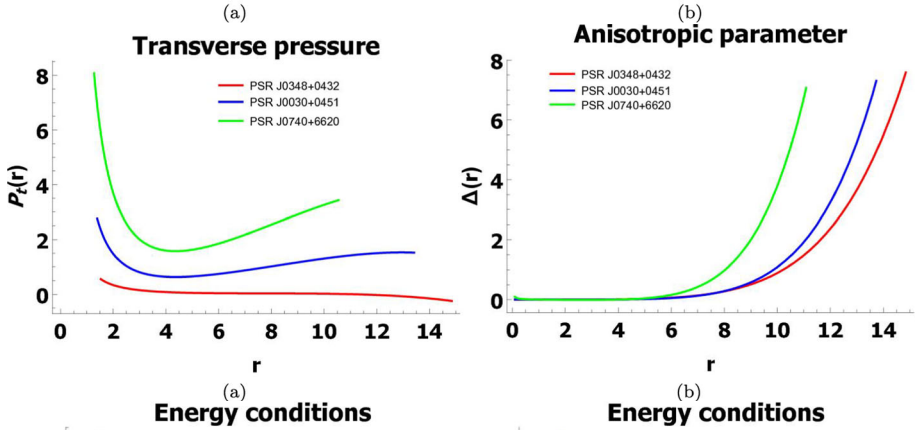

Fig. 2 Relationship of transverse pressure and anisotropic parameter w.r.t radial coordinate r. Observations of 3 pulsar

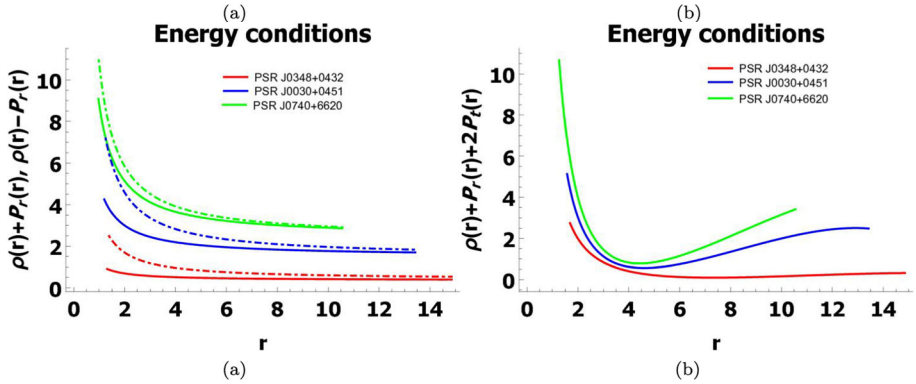

Fig. 3 Relationship of energy conditions w.r.t radial coordinate r. Observations of 3 pulsar (in **a** solid lines are of $\rho(r) + P_r(r)$ and dotted lines are of $\rho(r) - P_r(r)$)

stars is defined as,

$$\rho_c = \rho(r = 0) = a > 0. \tag{47}$$

After that the pressure at center of celestial dense star represented in our model is stated as,

$$p_c = p(r = 0) = \alpha a^2 > 0. \tag{48}$$

The above-mentioned data shows that ρ_c and p_c are positive inside celestial star configuration. On the contrary, at the celestial star boundary the $p_t > 0$ and physically attainable. Additionally, it can be seen from Figs. 1 and 2 that the anisotropic factor is regularly increasing function and it remains finite when we goes from center of star to the boundary. The Δ is regular at inner and repulsive in nature.

- **The regularity of the extrinsic curvature:**
The regularity of extrinsic curvature w.r.t hyper surface along exterior outline of celestial configuration provides the following relation

$$(p_r)_{r=R_s} = 0 \tag{49}$$

- **The non negative energy conditions:**
In discussion of energy conditions, the key tools allows us to study the typical and geodesic spacetime strictly. The energy conditions are tested by [19]. Which explains the act of association with gravity, spacetime, timelike and lightlike curves. While with conditions are Null, Weak, Strong, Dominant and Trace energy condition
$NECif\rho + p_k \geq 0, \forall k$
. $WECif\rho \geq 0, \rho + p_k \geq 0, \forall k$
. $SECif\rho + p_k \geq 0, \rho + \sum_k p_k \geq 0, \forall k$
. $DECif\rho \geq 0, \rho \pm p_k \geq 0, \forall k$
. $TECif\rho - p_k \geq 0, \rho - \sum_k p_k \geq 0, \forall k.$
The $k = r, t$. The positive form of state variables are plotted in Figs. 3 and 4 rapidly attached to the NEC, WEC

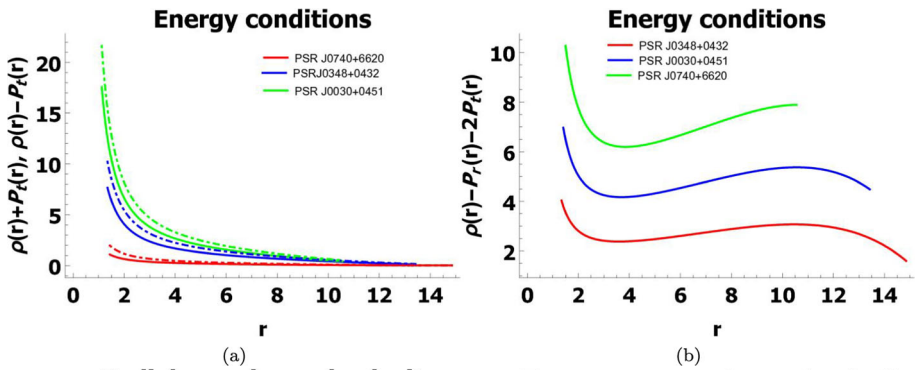

Fig. 4 Relationship of energy conditions w.r.t radial coordinate r. Observations of 3 pulsar (in **a** solid lines are of $\rho(r) + P_t(r)$ and dotted lines are of $\rho(r) - P_t(r)$)

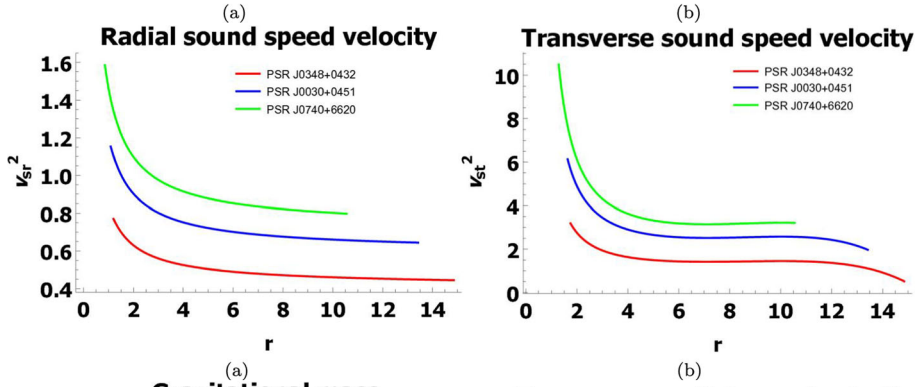

Fig. 5 Relationship of radial and transverse velocity w.r.t radial coordinate r. Observations of 3 pulsar

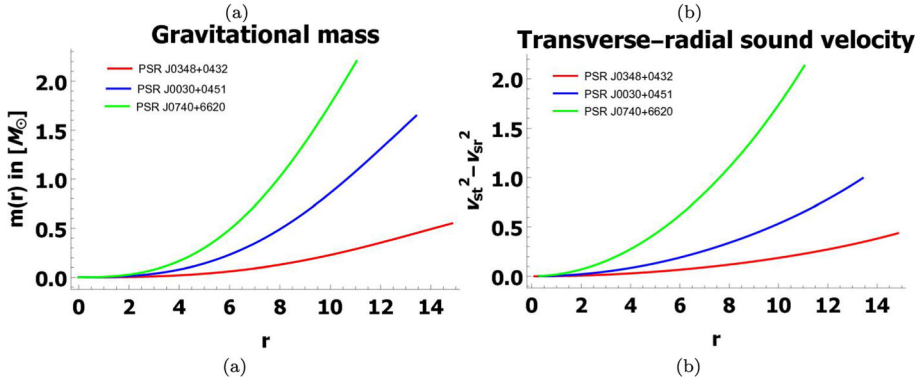

Fig. 6 Relationship of gravitational mass and $V_{sr} - V_{st}$ w.r.t radial coordinate r. Observations of 3 pulsar

and SEC. Where NEC derives that a viewer crossing a null plan will find the usual matter density as positive. As claimed by WEC, the matter density obtained by viewer passing by time-like plot is not varying, positive and connected to SEC. The sketch of flowing tensor assessed by associated viewer is non negative. The positive development attached with DEC and TEC is compatible with the 4th and 5th conditions, in which the DEC presents the mass and energy relation that will be unseen to flow rapid than light. By TEC, the stress-energy tensor outline should be compulsorily non negative based on metric conventions. From Figs. 3 and 4, all energy conditions are strictly tested which give results in non-exotic matter which fulfills celestial star configuration. Also, this model is well-behaved and achievable.

- **Collapsing ways of anisotropic celestial star stability:** It is hoped that the velocity of sound will be low than the speed of light inside celestial star. The relation of square of radial is $v_{sr}^2 = \frac{dp_r}{d\rho}$. The equation of transverse velocity of sound is $v_{st}^2 = \frac{dp_t}{d\rho}$. Where both of them must satisfy the causality conditions like $0 \leq v_{sr}^2 \leq 1$ and $0 \leq v_{st}^2 \leq 1$. According to Figs. 5 and 6b we can see that overall inner of stellar form, the v_{sr}^2 and v_{st}^2 are low then speed of light which is equal to 1and this fulfills the usual conditions. It is noticed that the variation in speed velocity reduces but causality is not contravene in dense objects.

6 Compactness factor and gravitational red-shift

Our stellar stars model explains the compactness factor as a dimensionless variable u. The u defines the relationship between mass and radius that is not arbitrarily vast. The compactification factor u of celestial stars for a 4D fluid sphere must be less then $\frac{2M}{R} < \frac{8}{9} \approx 0.8888$ [51]. Hence, it is admirable to test the gravitational mass function for celestial model given in Eq (14). From Eq. (14) the following

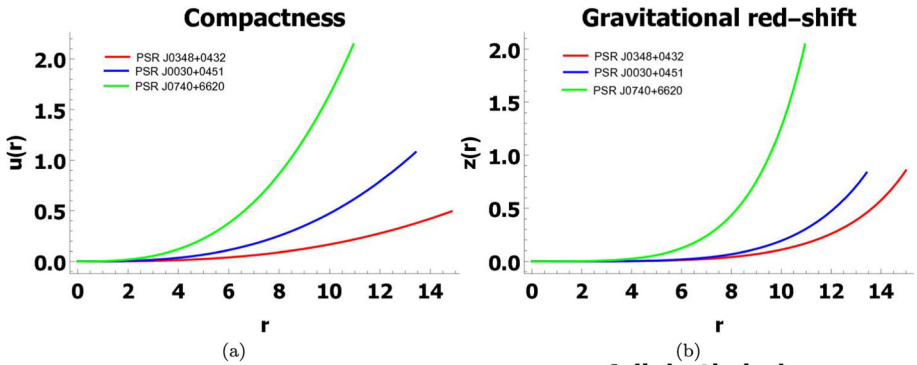

(a) (b)

Fig. 7 Relationship of compactness and red-shift parameter w.r.t radial coordinate r. Observations of 3 pulsar

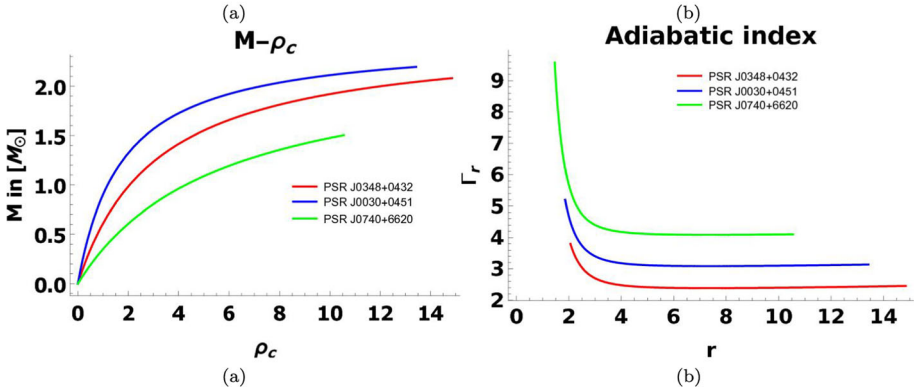

(a) (b)

Fig. 8 Relationship $M-\rho_c$ and Γ_r w.r.t radial coordinate r. Observations of 3 pulsar

equation of u is formulated as,

$$u(x) = \frac{m(x)}{\sqrt{x}}. \tag{50}$$

Wherefore, the red-shift in this work is related to u and asserted as,

$$Z(x) = \frac{1}{\sqrt{1-2u(x)}} - 1. \tag{51}$$

The geometry of gravitational mass equation $m(x)$, the compactification relation $u(x)$ and the red-shift $z(x)$ are plotted in Figs. 6a and 7. The graph presents that these 3 equations are gradually increasing w.r.t coordinate r and positive inside the dense stars. Also, they all are regular at the center of stars. When mass function increase, the compactification factor also increase.

7 Motionless stability and M-R figure

To this point, we initiate by talking about stability of celestial star structures depending on radial disturbance. The simplified form of stability rule is given by [52] and mentioned below,

$$\frac{\partial M}{\partial \rho_c} > 0 (\rightarrow stable\ configuration) \tag{52}$$

$$\frac{\partial M}{\partial \rho_c} < 0 (\rightarrow unstable\ configuration) \tag{53}$$

The total mass function is calculated as

$$M(\rho_c) = \frac{3R^3}{2}\left(\frac{\rho_c}{9+2R^2\rho_c}\right) \tag{54}$$

Figure 8a presents the difference of mass w.r.t central density. This give rise to solutions that extended the central density and presents its stability. Because of this, the range of ρ_c favors the mass saturation's. The increase in value of central density enhances the stability.

8 Adiabatic index

The specific heat equation which is also called the adiabatic index (Γ) is used to test the stability of model in a more efficient way. Here we used the following expression to check the reliability of this model.

$$\Gamma_r = \frac{\rho + p_r}{p_r}\frac{\partial p_r}{\partial \rho}. \tag{55}$$

Chandrasekhar [53] provided the information that the most convenient method to evaluate the stability of self gravitating fluid depends upon the adiabatic index. Bondi [54] mentioned the stability condition $\Gamma_r > \frac{4}{3}$ for newtonian isotropic sphere and $\Gamma_r = \frac{4}{3}$ for neutral stability. From [55] and [56] it can be seen that the adiabatic index is a sufficient condition to testify the stability of anisotropic fluid distribution. The stability results are achieved in Fig. 8b.

Table 1 Constant values for realistic star $PSRJ0348+0432$

PSR	b	a	α	β	γ	R [km]	$M[M_{\odot}]$
Density (ρ)	0.002	4.005	0.01	1.22	1	$14.85^{+0.11}_{-0.11}$	$2.01^{+0.04}_{-0.04}$
01 radial pressure (p_r)	−0.0001	−2.0015	0.070	−0.13711	1	$14.85^{+0.11}_{-0.11}$	$2.01^{+0.04}_{-0.04}$
Tangential pressure (p_t)	0.0000001	−2.0015	0.40	0.13711	1	$14.85^{+0.11}_{-0.11}$	$2.01^{+0.04}_{-0.04}$
Mass (m)	0.002	0.79	0.01	1.22	1	$14.85^{+0.11}_{-0.11}$	$2.01^{+0.04}_{-0.04}$
Red-shift (z)	−0.0000003	0.00001	0.01	1.22	1	$14.85^{+0.11}_{-0.11}$	$2.01^{+0.04}_{-0.04}$
Comactification factor (u)	0.002	4.005	0.01	1.22	1	$14.85^{+0.11}_{-0.11}$	$2.01^{+0.04}_{-0.04}$
Anisotropy (Δ)	15.00001;	−0.0015	20.40	0.01711	1	$14.85^{+0.11}_{-0.11}$	$2.01^{+0.04}_{-0.04}$
Radial velocity (v_{sr})	−0.0001	−3.0015	−0.070	0.22	1	$14.85^{+0.11}_{-0.11}$	$2.01^{+0.04}_{-0.04}$
Transverse velocity (v_{st})	−0.00001	22.9	40.90	1.22	1	$14.85^{+0.11}_{-0.11}$	$2.01^{+0.04}_{-0.04}$
Adiabatic index (Γ_r)	−0.008	−3.0015	−0.070	0.001	1	$14.85^{+0.11}_{-0.11}$	$2.01^{+0.04}_{-0.04}$

Table 2 Constant values for realistic star $PSRJ0030+0451$

PSR	b	a	α	β	γ	R [km]	$M[M_{\odot}]$
Density (ρ)	0.002	5.0015	0.01	1.22	1	$13.42^{+0.24}_{-0.22}$	$2.14^{+0.10}_{-0.09}$
Radial pressure (p_r)	− 0.0001	− 2.9015	0.050	− 0.12611	1	$13.42^{+0.24}_{-0.22}$	$2.14^{+0.10}_{-0.09}$
Tangential pressure (p_t)	0.0000001	− 2.0015	0.30	0.13711	1	$13.42^{+0.24}_{-0.22}$	$2.14^{+0.10}_{-0.09}$
Mass (m)	0.002	0.69	0.01	1.22	1	$13.42^{+0.24}_{-0.22}$	$2.14^{+0.10}_{-0.09}$
Red-shift (z)	− 0.0000002	0.0000015	0.01	1.22	1	$13.42^{+0.24}_{-0.22}$	$2.14^{+0.10}_{-0.09}$
Comactification factor (u)	0.002	5.0015	0.01	1.22	1	$13.42^{+0.24}_{-0.22}$	$2.14^{+0.10}_{-0.09}$
Anisotropy (Δ)	0.00001	− 0.0015	10.40	0.01711	1	$13.42^{+0.24}_{-0.22}$	$2.14^{+0.10}_{-0.09}$
Radial velocity (v_{sr})	− 0.0001	− 6.015	− 0.050	0.22	1	$13.42^{+0.24}_{-0.22}$	$2.14^{+0.10}_{-0.09}$
Transverse velocity (v_{st})	− 0.00001	22.92	41.01	1.22	1	$13.42^{+0.24}_{-0.22}$	$2.14^{+0.10}_{-0.09}$
Adiabatic index (Γ_r)	− 0.006	− 6.015	− 0.050	0.0001	1	$13.42^{+0.24}_{-0.22}$	$2.14^{+0.10}_{-0.09}$

Table 3 Constant values for realistic star $PSRJ0740+6620$

PSR	b	a	α	β	γ	R [km]	$M[M_{\odot}]$
Density (ρ)	0.0001	6.002	0.01	1.22	1	$10.55^{+0.41}_{-0.40}$	$1.14^{+0.15}_{-0.14}$
Radial pressure (p_r)	− 0.0001	− 2.605	0.120	− 0.21311	1	$10.55^{+0.41}_{-0.40}$	$1.14^{+0.15}_{-0.14}$
Tangential pressure (p_t)	0.0000001	− 2.0015	0.40	0.13711	1	$10.55^{+0.41}_{-0.40}$	$1.14^{+0.15}_{-0.14}$
Mass (m)	0.002	0.59	0.01	1.22	1	$10.55^{+0.41}_{-0.40}$	$1.14^{+0.15}_{-0.14}$
Red-shift (z)	− 0.000001	0.00002	0.01	1.22	1	$10.55^{+0.41}_{-0.40}$	$1.14^{+0.15}_{-0.14}$
Comactification factor (u)	0.0001	6.002	0.01	1.22	1	$10.55^{+0.41}_{-0.40}$	$1.14^{+0.15}_{-0.14}$
Anisotropy (Δ)	0.0000003	− 0.0015	12.50	0.2711	1	$10.55^{+0.41}_{-0.40}$	$1.14^{+0.15}_{-0.14}$
Radial velocity (v_{sr})	− 0.0001	− 3.05	− 0.120	0.22	1	$10.55^{+0.41}_{-0.40}$	$1.14^{+0.15}_{-0.14}$
Transverse velocity (v_{st})	− 0.00001	22.87	40.61	1.22	1	$10.55^{+0.41}_{-0.40}$	$1.14^{+0.15}_{-0.14}$
Adiabatic index (Γ_r)	− 0.002	− 3.05	− 0.120	0.001	1	$10.55^{+0.41}_{-0.40}$	$1.14^{+0.15}_{-0.14}$

9 Conclusions and discussions

The interesting aspects of this wok are based on testing the possible new well-organized group of anisotropic stars that results form viable dense static symmetric configurations in place of NSs. With this in mind, we used a modified form of non linear vdw EoS, which shows the relationship between radial pressure, density and constants like α, β and γ. Together with a gravitational potential ($Z(x)$) as developing function over an anisotropic matter dispensation that

forms the grounds for stellar configurations. This research work shows uniform, achievable, and stable model inebriated by parameters involved in EoS. An important observation is that the expected radii for noticed pulsars are efficiently obtained from the continuity of the 2nd fundamental form with the highly spotted mass and coordinating radii are attained by fine alteration of parameters extracted from theory. The graphical results of this study are clearly discussed. In Figs. 1 and 2a, the ρ, p_r and p_t decrease gradually, regular and are non-negative. Figure 2b graphically shows that anisotropic parameter known as $\Delta(r)$ increase uniformly. Plus, it can be seen that the anisotropy factor has lower value close to the center and it starts rising continuously while moving away from the center. The behaviour of energy conditions show the continuity and stability while decreasing in Figs. 3 and 4. According to Fig. 5 the square of radial and transverse sound speed is positively reducing along x-axis and both are stable. Additionally, the relationship between them is clearly plotted in Fig. 6b which shows their increasing behaviour along all 3 pulsars. Further, $m(r)$, $u(r)$ and $z(r)$ plotted in Figs. 6a and 7 explained balanced, regular, positive and increasing behaviour. The compactification factor $u(r)$ defines the dense objects in different groups. Now, coming to Fig. 8a of M in $[M_{\odot}]$ along ρ_c exhibit steady growing manner. Figure 8b is plotted for adiabatic index that satisfies the given condition Eq. (55) which shows the stability of our model. All the algebraic and graphical study of pulsar $PSRJ0348+0432$, $PSRJ0030+0451$ and $PSRJ0740+6620$ involving different constants $(a, b, \alpha, \beta, \gamma)$ and parameters displays a well behaving, positive, uniform and stable model. Table 1 shows the different parametric values for pulsar $PSRJ0348+0432$ and taking values of R (km) and $[M_{\odot}]$ as $14.85^{+0.11}_{-0.11}$ and $2.01^{+0.04}_{-0.04}$, respectively. For pulsar $PSRJ0030+0451$ the constant values are listed in Table 2, where R (km) and $[M_{\odot}]$ are $13.42^{+0.24}_{-0.22}$ and $2.14^{+0.10}_{-0.09}$. Accordingly, Table 3 have parametric values of $PSRJ0740+6620$ by considering R (km) and $[M_{\odot}]$ as $10.55^{+0.41}_{-0.40}$ and $1.14^{+0.15}_{-0.14}$. Existence of overhead specified conditions presents a physically adequate anisotropic spherically symmetric model with modified vdw EoS for three different pulsars coming from interior of neutron dense objects. In the end, it is important to discuss that this model accepts every useful graphical and algebraic information of dense objects. Also give environmental proof of evaluation of static celestial configuration that is examined in high density area. This study encourage the testament of realistic pulsars.

Data Availability Statement My manuscript has no associated data. [Authors' comment: Data sharing not applicable to this article as no datasets were generated or analysed during the current study.]

Code Availability Statement My manuscript has no associated code/software. [Authors' comment: Code/Software sharing not applicable to this article as no code/software was generated or analysed during the current study.]

Funded by SCOAP[3].

References

1. S. Chandrasekhar, The highly collapsed configurations of a stellar mass. Mon. Not. Roy. Astron. Soc. **95**, 207 (1935)
2. J.R. Oppenheimer, G.M. Volkoff, On massive neutron cores. Phys. Rev. **55**, 374 (1939)
3. D.J. Wentzel, On the shape of magnetic stars. Astrophys. J. **133**, 170 (1961)
4. J. Kumar, S.K. Maurya, A.K. Prasad, A. Banerjee, Relativistic charged spheres: compact stars, compactness and stable configurations. J. Cosmol. Astropart. Phys. **2019**, 005 (2019). arXiv:1804.01779 [gr-qc]
5. J. Kumar, P. Bharti, Relativistic models for anisotropic compact stars: a review. New Astron. Rev. **95**, 101662 (2022)
6. A. Alho, J. Natário, P. Pani, G. Raposo, Compact elastic objects in general relativity. Phys. Rev. D **105**, 2470 (2022). arXiv:2107.12272 [gr-qc]
7. A.V. Astashenok, S.D. Odintsov, V.K. Oikonomou, Compact stars with dark energy in general relativity and modified gravity. Phys. Dark Univ. **42**, 101295 (2023). arXiv:2307.14862 [gr-qc]
8. P. Candelas, Vacuum polarization in Schwarzschild spacetime. Phys. Rev. **21**, 2185 (1980)
9. P. Candelas, K.W. Howard, vacuum in Schwarzschild space-time. Phys. Rev. D **29**, 1618 (1984)
10. K. Schwarzschild, On the gravitational field of a mass point according to Einstein's theory. J. Math. Phys. **1916**, 189 (1999). arXiv:physics.hist-ph/9905030
11. J. Ponce de Leon, Stellar models with Schwarzschild and non-Schwarzschild vacuum exteriors. Gravit. Cosmol. **14**, 65 (2008). arXiv:0711.0998 [gr-qc]
12. H. Crater, Is the Schwarzschild metric a vacuum solution of the Einstein equation? (2014). arXiv:1106.2040 [gr-qc]
13. C. Cataldo, On the Schwarzschild solution: a review. Int. J. Adv. Eng. Sci. **4**, 2349 (2017)
14. G. Weinstein, A comprehensive survey of Schwarzschild's original papers: Schwarzschild's trick and Einstein's s(h)tick. (2023). arXiv:2312.01865 [physics.hist-ph]
15. M. Malaver, Regular model for a quark star with Van der Waals modified equation of state. World Appl. Progr. **3**, 309 (2013)
16. R.C.S. Jantsch, M.H.B. Christmann, G.M. Kremer, The van der Waals fluid and its role in cosmology. Int. J. Mod. Phys. D **25**, 1650031 (2016). arXiv:1601.05337 [gr-qc]
17. G.M. Kontogeorgis, R. Privat, J. Jaubert, Taking another look at the van der Waals equation of state-almost 150 years later. J. Chem. Eng. Data **64**, 4619 (2019)

18. R. Fleming, General relativity as a quantum Van der Waals torque effect. Glob. Strateg. J. **101**, 14850 (2019)
19. A. Errehymy, G. Mustafa, Y. Khedif, M. Daoud, H.I. Alrebdi, A. Abdel-Aty, Self-gravitating anisotropic model in general relativity under modified Van der Waals equation of state: a stable configuration. Eur. Phys. J. C **82**, 455 (2022)
20. A. Ditta, X. Tiecheng, A. Errehymy, G. Mustafa, S.K. Maurya, Anisotropic charged stellar models with modified Van der Waals EoS in f(Q) gravity. Eur. Phys. J. C **83**, 254 (2023)
21. G. Mustafa, F. Javed, S.K. Maurya, S. Ray, Possibility of stable thin-shell around wormholes within the string cloud and quintessential field via the Van der Waals and polytropic EOS in general relativity. Chin. J. Phys. **88**, 0577 (2024). arXiv:2211.10778 [gr-qc]
22. J.M. Lattimer, M. Prakash, The physics of neutron stars. Science **304**, 536 (2004)
23. T. Damour, 1974, the discovery of the first binary pulsar. Class. Quantum Gravity **32**, 1361 (2015). arXiv:1411.3930 [gr-qc]
24. B. Burnell, Jocelyn, The past, present and future of pulsars. Nat. Astron. **1**, 831 (2017)
25. A. Mann, The golden age of neutron-star physics has arrived. Nature **579**, 20 (2020)
26. C.J. Zhang, Z.H. Shang, W.M. Chen, L. Xie, X.H. Miao, A review of research on pulsar candidate recognition based on machine learning. Procedia Comput. Sci. **166**, 534 (2020)
27. D.J. Reardon, M. Bailes, R.M. Shannon, C. Flynn, J. Askew, N.D.R. Bhat et al., The neutron star mass, distance, and inclination from precision timing of the brilliant millisecond pulsar J0437–4715. Astrophys. J. Lett. **971**, 2041 (2024). arXiv:2407.07132 [astro-ph.HE]
28. D. Farrell, F. Weber, M.G. Orsaria, I.F.R. Sandoval, M. Canullán, R. Negreiros, Fast pulsars, neutron stars, and astrophysical strange quark matter objects. (2024). arXiv:2402.08835 [astro-ph.HE]
29. L. Herrera, G. Ruggeri, L. Witten, Adiabatic contraction of anisotropic spheres in general relativity. Astrophys. J. **234**, 1094 (1979)
30. L. Herrera, J. Jiménez, L. Leal, J. Ponce de León, M. Esculpi, V. Galina, Anisotropic fluids and conformal motions in general relativity. J. Math. Phys. **25**, 3274 (1984)
31. L. Herrera, N.O. Santos, Local anisotropy in self-gravitating systems. Phys. Rep. **286**, 53 (1997)
32. H. Hernandez, L.A. Nunez, Nonlocal equation of state in anisotropic static fluid spheres in general relativity. Can. J. Phys. **82**, 29 (2002). arXiv:gr-qc/0107025
33. S.K. Maurya, Y.K. Gupta, Charged fluid to anisotropic fluid distribution in general relativity. Astrophys. Space Sci. **344**, 243 (2013)
34. A. Sah, P. Chandra, Spherical anisotropic fluid distribution in general relativity. World J. Mech. **6**, 487 (2016)
35. P. Boonserm, T. Ngampitipan, M. Visser, Modelling anisotropic fluid spheres in general relativity. Int. J. Mod. Phys. D **25**, 1650019 (2016). arXiv:1501.07044 [gr-qc]
36. F. Tello-Ortiz, S. Maurya, A. Errehymy, K. Newton Singh, M. Daoud, Anisotropic relativistic fluid spheres: an embedding class I approach. Eur. Phys. J. C **79**, 209 (2019)
37. L. Herrera, Stability of the isotropic pressure condition. Phys. Rev. D **101**, 104024 (2020). arXiv:2005.06358 [gr-qc]
38. M. Cadoni, A.P. Sanna, M. Tuveri, Anisotropic fluid cosmology: an alternative to dark matter? Phys. Rev. D **102**, 023514 (2020). arXiv:2002.06988 [gr-qc]
39. N.F. Naidu, S. Carloni, P. Dunsby, On anisotropic two-fluid stellar objects in general relativity. Phys. Rev. D **106**, 2470 (2022). arXiv:2210.06867 [gr-qc]
40. K.C. Gendreau, Z. Arzoumanian, T. Okajima, The Neutron star Interior Composition ExploreR (NICER): an explorer mission of opportunity for soft X-ray timing spectroscopy. Space Telesc. Instrum. **8443**, 8 (2012)
41. K.C. Gendreau, Z. Arzoumanian, W.A. Phillip, L.A. Cheryl, F.A. John, A. Andrew et al., The Neutron star Interior Composition Explorer (NICER): design and development. Space Telesc. Instrum. **9905**, 16 (2016)
42. S. Bogdanov, W.C.G. Ho, T. Enoto, S. Guillot, A.K. Harding, G.K. Jaisawal et al., Neutron Star Interior Composition Explorer X-ray timing of the radio and X-ray quiet pulsars PSR J1412+7922 and PSR J1849–0001. Astrophys. J. **877**, 8 (2019). arXiv:1902.00144 [astro-ph.HE]
43. N. Yunes, M.C. Miller, K. Yagi, Gravitaional-wave and X-ray probes of the neutron star equation of state. Nat. Rev. Phys. **4**, 237 (2022)
44. C. Devarshi, L.W. Anna, J.D. Alexander, M.C. Miller, S.M. Morsink, T. Salmiet al., Exploring waveform variations among neutron star ray-tracing codes for complex emission geometries. (2024). arXiv:2406.07285 [astro-ph.HE]
45. S. Rahman, M. Visser, Spacetime geometry of static fluid spheres. Class. Quantum Gravity **19**, 935 (2002). arXiv:gr-qc/0103065
46. K. Lake, All static spherically symmetric perfect-fluid solutions of Einstein's equations. Phys. Rev. D **67**, 10 (2003)
47. L. Herrera, J. Ospino, A. Di Prisco, All static spherically symmetric anisotropic solutions of Einstein's equations. Phys. Rev. D **77**, 027502 (2008). arXiv:0712.0713 [gr-qc]
48. S.A. Mardana, I. Noureenb, A. Khalid, Charged anisotropic compact star core-envelope model with polytropic core and linear envelope. Eur. Phys. J. C **81**, 912 (2021)
49. S. Capozziello, V.F. Cardone, S. Carloni, S. De Martino, M. Falanga, A. Troisi et al., Constraining Van der Waals quintessence by observations. J. Cosmol. Astropart. Phys. **0504**, 005 (2005). arXiv:astro-ph/0410503
50. S. O'brien, J.L. Synge, Jump conditions at the discontinuties in general relativity. Commun. Dublin Inst. Adv. Stud. A **9**, 20 (1952)
51. H.A. Buchdahl, General relativistic fluid spheres. Phys. Rev. **116**, 1027 (1959)
52. B.K. Harrison, K.S. Thorne, M. Wakano, J.A. Wheeler, *Gravitational Theory and Gravitational Collapse*, vol. 194 (University of Chicago Press, Chicago, 1965), p.177
53. S. Chandrasekhar, The dynamical instability of gaseous masses approaching the Schwarzschild limit in general relativity. Astrophys. J. **140**, 417 (1964)
54. H. Bondi, The contraction of gravitating spheres. Proc. Roy. Soc. Lond. A **281**, 39 (1964)
55. R. Chan, L. Herrera, N.O. Santos, Dynamical instability in the collapse of anisotropic matter. Class. Quantum Gravity **9**, L133 (1992)
56. R. Chan, L. Herrera, N.O. Santos, Dynamical instability for radiating anisotropic collapse. Mon. Not. Roy. Astron. Soc. **265**, 533 (1993)